JOURNAL OF MATERIALS SCIENCE **35** (2000) 323–329

Crystallization kinetics and structure of (TeO_2-TiO_2-Fe_2O_3) Glasses

I. SHALTOUT
Physics Department, Faculty of Science, UAE University, AL-Ain 17551, UAE
E-mail: I.Shaltout@nyx.uaeu.ac.ae

Crystallization kinetics and structure of ($85TeO_2 + 15TiO_2$) and ($85TeO_2 + 10TiO_2 + 5Fe_2O_3$) glasses are studied using differential scanning calorimetry DSC, IR spectroscopy and XRD. DSC curves in the temperature range from 50 to 525 °C with different heating rates from 10 to 40 °C/min are used to study the crystallization behavior of the glasses and effects of different heating rates on the glass transition and crystallization temperatures (T_g and T_p). The activation energies of the glass transition and crystallization processes were determined from the shift of T_g and T_p with the heating rates using Kissinger's formula. Effects of the polymorphic nature of TeO_2 on the crystallization mechanisms are discussed and the phases crystallized during the DSC process were identified by XRD. IR spectra in the frequency range (500–4000 cm^{-1}) are measured and possible coordination states of the constituent oxides are discussed for heat-treated and untreated glasses.

1. Introduction

TeO_2-Based glasses are important materials for many possible electrical and optical applications [1–4]. The addition of transition metal ions (TMI) to these glasses produces important materials in uses as elements in memory switching devices and cathode materials for batteries [5, 6]. Many studies on crystallization kinetics, thermal analysis, Raman spectra, X-ray photoelectron spectroscopy and structure of TeO_2-based glasses have been reported recently [7–9]. Nevertheless, crystallization kinetics studies on Tellurite glasses in general, to the best of our knowledge, are limited to a few papers [10–12].

In a previous work the present author and coworkers have studied the structure and thermal properties of (TeO_2-WO_3) glasses by Raman spectroscopy, differential scanning calorimetry (DSC) and FTIR spectra in the range (150–24000 cm^{-1}) [2, 4]. In the present work, crystallization kinetics and structure of ($85TeO_2 + 15TiO_2$) and ($85TeO_2 + 10TiO_2 + 5Fe_2O_3$) glasses are studied using DSC, IR spectra and X-ray diffraction.

2. Experimental procedures

Glasses were prepared by fusing appropriate mixtures of reagent grade TeO_2, TiO_2, and Fe_2O_3 (Alfa Johnson Mathey electronics 99.995%) in a platinum crucible at 900 °C for 30 min. The melt was frequently stirred to insure complete homogeneity of the sample, and after complete fusion the melt was poured as quickly as possible on a stainless steel plate at room temperature. Bulk samples of about 3 cm diameter and 0.3–0.4 mm thickness were obtained. Glass samples have not been subjected to any annealing process and its amorphous state was confirmed by X-ray diffraction (XRD) using CuK_α radiation (Philips Analytical X-ray B. V type PW 1840 instrument, PC-APD diffraction software).

DSC measurements were carried out using a Perkin Elmer DSC7 instrument with nitrogen flow at a rate of 50 ml/min. The instrument has been calibrated before measurements using standard curves of In and Zn. Measurements have been carried out in the temperature range (50–525 °C) with different heating rates from 10 to 40 °C/min. Glasses were carefully ground and an amount of 5 mg powdered sample was kept the same for all measurements. FTIR spectra of the glasses in the range 400–1000 cm^{-1} with a resolution of 2 cm^{-1} were collected for powders dispersed in KBr pallets using a (Shimatsu FTIR model DR-8001 instrument). To identify the crystalline phases developed upon different heat treatment processes, samples were heat treated at 460 °C (the first crystallization peak) and at 500 °C (the second crystallization peak) for 30 min and the crystallized phases have been identified by XRD.

3. Results and discussions

Fig. 1 shows the normalized DSC curves of ($85TeO_2 + 15TiO_2$) glasses in the temperature range 50–525 °C with different heating rates ϕ from 10–40 °C/min. A broad endothermic transformation, corresponding to the glass transition temperature T_g, is observed and followed by two or three crystallization peaks T_p due to successive crystallization processes. The sharp crystallization peaks observed here indicate that bulk crystallization is predominant [13–15]. As shown in Fig. 1 the endothermic transition is very

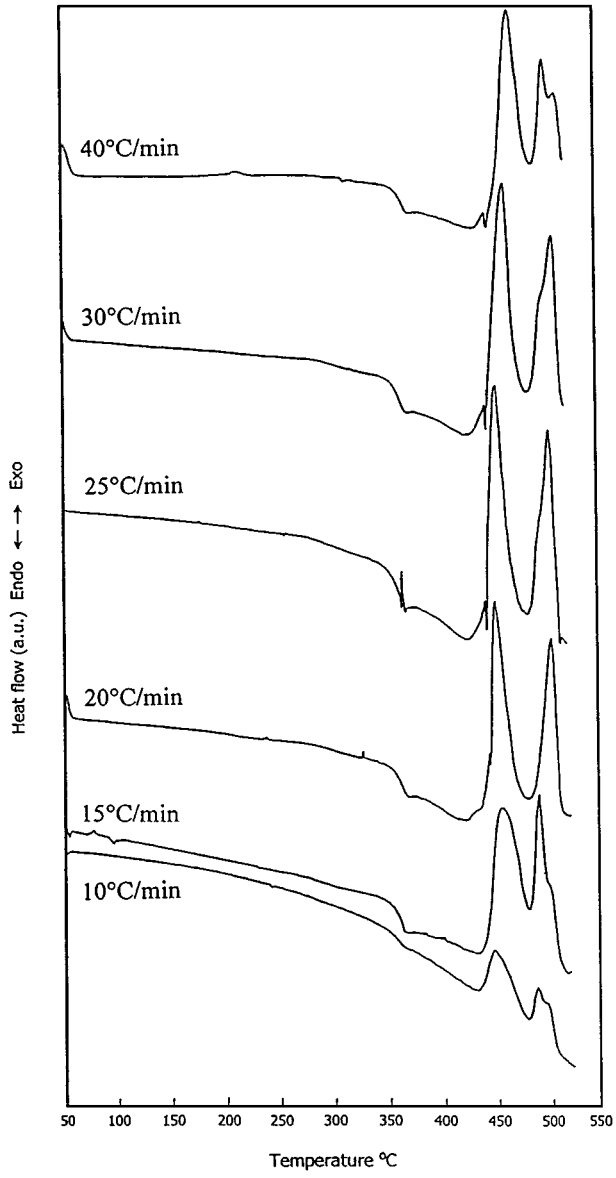

Figure 1 DSC curves of ($85TeO_2 + 15TiO_2$) glasses at different heating rates ($10 \leq \phi \leq 40\,^{\circ}$C/min).

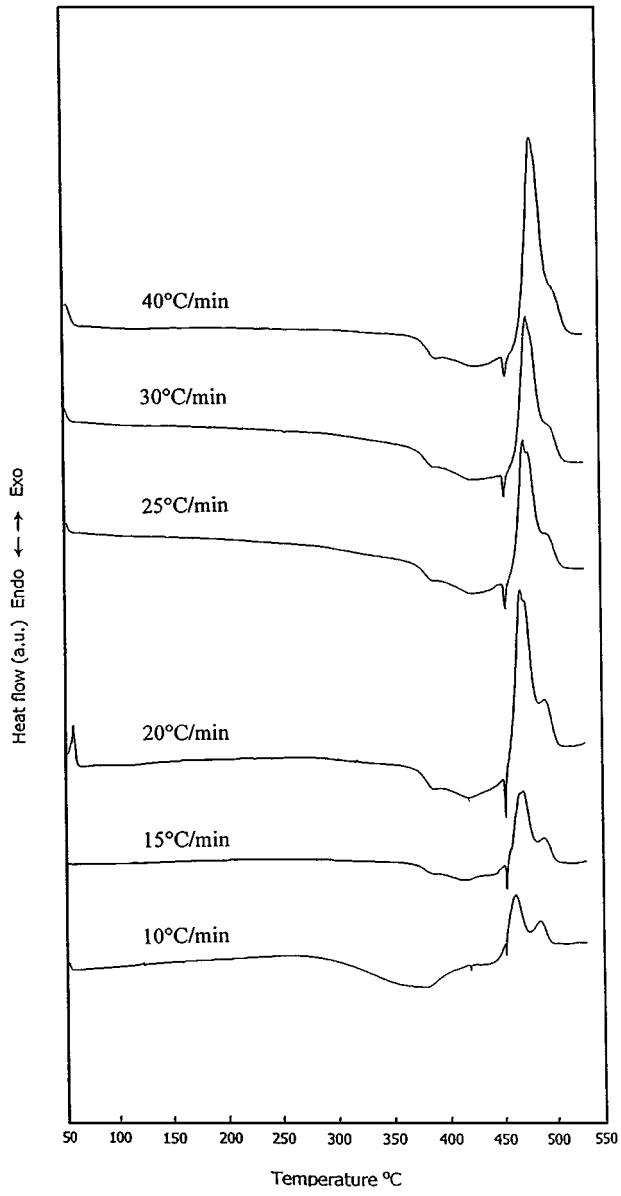

Figure 2 DSC curves of ($85TeO_2 + 10TiO_2 + 5Fe_2O_3$) glasses at different heating rates ($10 \leq \phi \leq 40\,^{\circ}$C/min).

broad for low heating rate ($\phi = 10\,^{\circ}$C/min), and it becomes more pronounced and well defined for high heating rates ($15 \leq \phi \leq 40\,^{\circ}$C/min). Fig. 2 shows the DSC curves of ($85TeO_2 + 10TiO_2 + 5Fe_2O_3$) glasses. The same characteristic features are observed, where T_g is followed by two crystallization peaks (T_{p1} and T_{p2}). Thermal parameters obtained from Figs 1 and 2 are summarized in Table I. The relative heights of the first and second crystallization peaks (T_{p1} and T_{p2}) and the area under these two peaks are comparable for glasses free of Fe_2O_3 as shown in Fig. 1.

The two main successive crystallization peaks observed in Figs 1 and 2 may be explained in view of the polymorphic nature of TeO_2 as follows. It is known that TeO_2 crystallizes as α-TeO_2 or β-TeO_2 [16], and the amorphous state of TeO_2-based glasses could be considered as assemblages of different clusters (radius ≤ 10 nm) with strained interfaces in between [17, 18]. Such interfaces are differently oriented and strained. That is, some of them are highly strained and others are of lower strained degree. On heating the sample up, the low strained interfaces could get enough energy at low temperature to relax and nucleate, and consequently, the first crystallization process starts at the first crystallization onset. As temperature increases beyond the first crystallization peak, the remaining highly strained interfaces between clusters start to relax, and as a result, a second crystallization process is observed. The third crystallization peak observed in the range of 500–518 °C depending on the heating rate for the glass without Fe_2O_3, as seen in Fig. 1, could be due to the phase separation of the ($TiTe_3O_8$) phase which has been identified by (XRD) for this sample after being heat treated at 500 °C for 30 min as shown in Fig. 7.

On comparison of Figs 1 and 2 it is observed that, due to the addition of Fe_2O_3 to these glasses, both T_g and T_{p1} have been shifted up by about 10 °C (as seen in Table I). Moreover, the second crystallization peak observed in the range of 481–497 °C in Fig. 2 has been significantly suppressed and gradually overlapped with the first crystallization peak as a result of increasing the heating rate from 10 to 40 °C/min. These changes

TABLE I Thermal parameters of ($85TeO_2 + 15TiO_2$) and ($85TeO_2 + 10TiO_2 + 5Fe_2O_3$) glasses

	($85TeO_2 + 15TiO_2$) Glasses				($85TeO_2 + 10TiO_2 + 5Fe_2O_3$) Glasses		
ϕ (°C/min)	T_g (°C)	T_{p1} (°C)	T_{p2} (°C)	T_{p3} (°C)	T_g (°C)	T_{p1} (°C)	T_{p2} (°C)
10	354	451	493	500		458	481
15	358	459	497	504	367	464	484
20	363	457		508	368	465	488
25	361	461	500	511	367	470	486
30	362	464	502	513	372	473	493
40	365	473	506	518	374	478	497

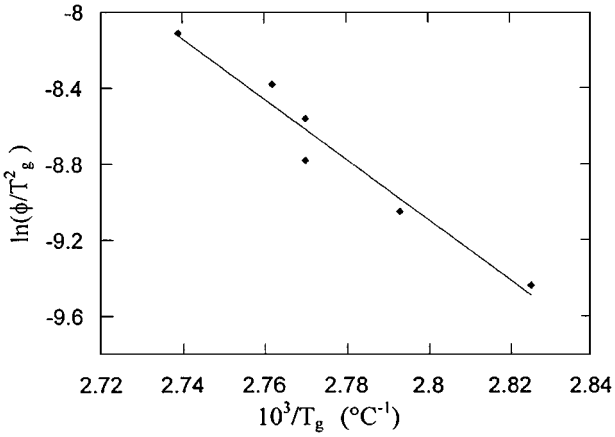

Figure 3 Plot of $\ln(\phi/T_g^2)$ vs. $10^3/T_g$ of ($85TeO_2 + 15TiO_2$) glasses.

suggest that Fe_2O_3 is acting as a crystallization inhibitor in these glasses [19, 20]. In terms of the strained interfaces explanation, the addition of Fe_2O_3 could increase the strain degree of the different interfaces and consequently inhibits crystallization at lower temperature (compared to the glass without Fe_2O_3). Therefore, the first crystallization process has occurred at a higher temperature while the second crystallization peak has been suppressed (as heating rate increases).

Fig. 3 shows a plot of $\ln(\phi/T_g^2)$ vs. $10^3/T_g$ for the ($85TeO_2 + 15TiO_2$) glasses. An activation energy of ($E_t = 129.7$ kJ/mol) for the glass transition process is obtained from the slope of this plot by using Kissinger's formula [21, 22]:

$$\ln(\phi/T_g^2) = -\frac{E_t}{RT_g} + \text{constant} \qquad (1)$$

where T_g is the glass transition temperature and ϕ is the heating rate. A similar expression:

$$\ln(\phi/T_p^2) = -\frac{E_c}{RT_p} + \text{constant} \qquad (2)$$

where T_p is the peak crystallization temperature, is often used to calculate the activation energy of the crystallization process E_c [21, 22]. It has been pointed out that Equation 2, in this simple form, is supposed to be used to calculate E_c only if nucleation and crystal growth are occurring separately as two successive processes [13, 21, 22]. For simultaneous occurring of nucleation and crystallization processes, equation 2 has been modified to the form:

$$\ln\left(\frac{\phi^n}{T_p}\right) = -\frac{mE_c}{RT_p} + \text{constant} \qquad (3)$$

where n is a constant known as Avrami parameter (order of crystallization reaction) and m is a constant represents the dimensionality of the crystallization growth.

In the present work, E_c for the different crystallization processes were calculated using equation 2, as simply applied by many authors [21–23] supposing that nucleation and crystallization are taking place separately as two successive processes. That is, the sample is well nucleated prior to crystallization and therefore crystallization occurs on a fixed number of nuclei at different heating rates.

Fig. 4 shows a plot of $\ln(\phi/T_p^2)$ vs. $10^3/T_p$ of the ($85TeO_2 + 15TiO_2$) glasses for the first, second and third crystallization peaks. The activation energies of crystallization ($E_{c1} = 94.8$ kJ/mol, $E_{c2} = 219.3$ kJ/mol, and $E_{c3} = 155.6$ kJ/mol) for these three crystallization processes are obtained using equation 2.

Figs 5 and 6 respectively show plots of $\ln(\phi/T_g^2)$ vs. $10^3/T_g$, and $\ln(\phi/T_p^2)$ vs. $10^3/T_p$ for ($85TeO_2 + 10TiO_2 + 5Fe_2O_3$) glasses. The activation energy of the glass transition process $E_t = 105.2$ kJ/mol and activation energies of the two crystallization processes ($E_{c1} = 112.2$ kJ/mol and $E_{c2} = 136.6$ kJ/mol) were calculated from these plots using equation 2. Activation energies of all glasses are summarized in Table II.

Fig. 7 shows the XRD of the untreated and heat-treated ($85TeO_2 + 15TiO_2$) glasses. As shown the XRD of the untreated glasses confirms its amorphous state. For the ($85TeO_2 + 15TiO_2$) glasses heat-treated at 460 °C for 30 min (the first crystallization peak temperature, for heating rate $\phi = 25$ °C/min), a single crystallized phase (Paratellurite TeO_2, in which Te atoms are four fold coordinated) is identified. For the sample heat-treated at 500 °C for 30 min (the second crystallization peak, for heating rate $\phi = 25$ °C/min and around the third crystallization peak), a Titanium-Tellurate ($TiTe_3O_8$) phase have been developed as shown in Fig. 7. These crystallized phases are corresponding to the successive crystallization peaks observed in the DSC curves as discussed above.

Fig. 8 shows the (XRD) of the untreated and heat-treated ($85TeO_2 + 10TiO_2 + 5Fe_2O_3$) glasses. As shown, the same crystallized phases are identified upon heat treatment of the glasses at 470 °C (the first crystallization peak temperature for heating rate

TABLE II Activation energies of the glass transition and crystallization processes

$(85TeO_2 + 15TiO_2)$ Glasses				$(85TeO_2 + 10TiO_2 + 5Fe_2O_3)$ Glasses		
E_t (kJ/mol)	E_{c1} (kJ/mol)	E_{c2} (kJ/mol)	E_{c3} (kJ/mol)	E_t (kJ/mol)	E_{c1} (kJ/mol)	E_{c2} (kJ/mol)
129.7	94.8	219.3	155.6	105.2	112.2	136.3

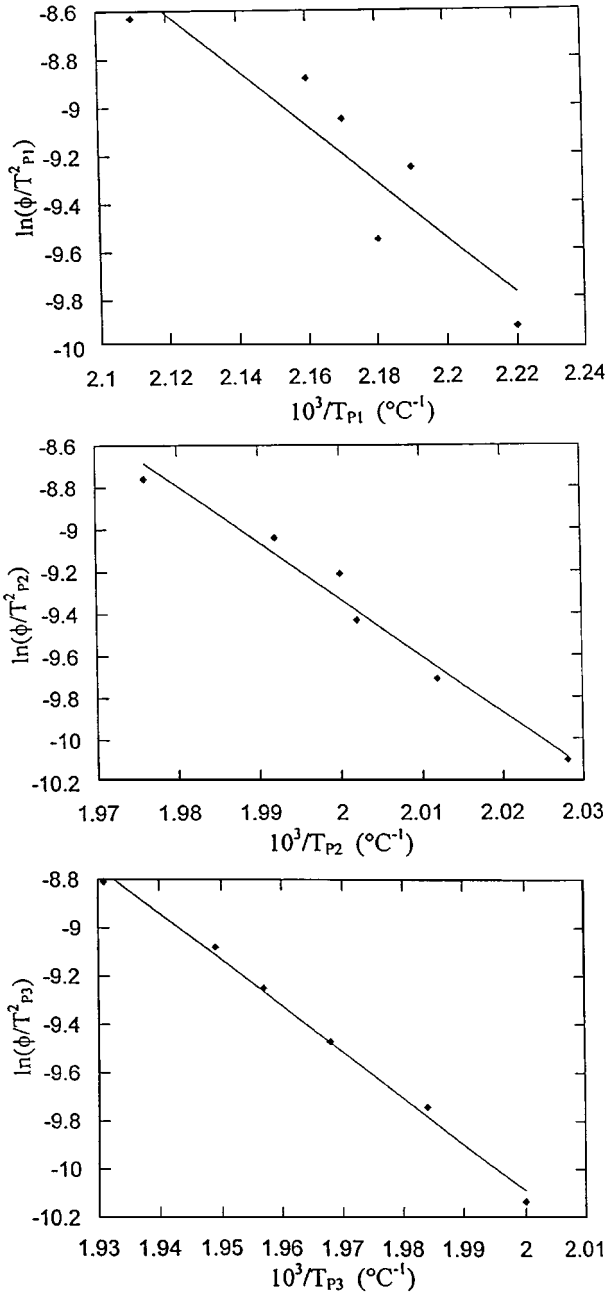

Figure 4 Plot of $\ln(\phi/T_p^2)$ vs. $10^3/T_p$ of $(85TeO_2 + 15TiO_2)$ glasses for the first, second, and third crystallization peaks (T_{p1}, T_{p2}, and T_{p3}).

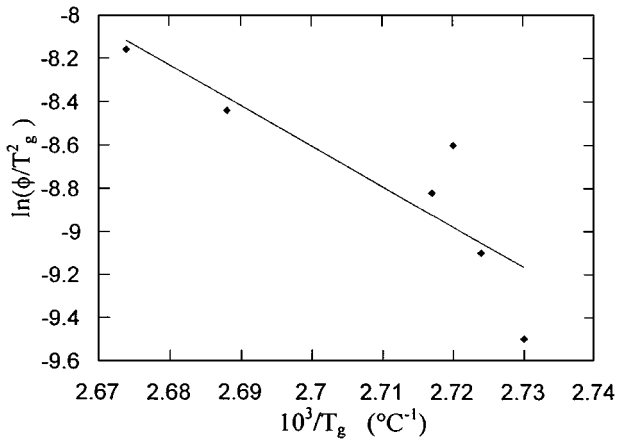

Figure 5 Plot of $\ln(\phi/T_g^2)$ vs. $10^3/T_g$ of $(85TeO_2 + 10TiO_2 + 5Fe_2O_3)$ glasses.

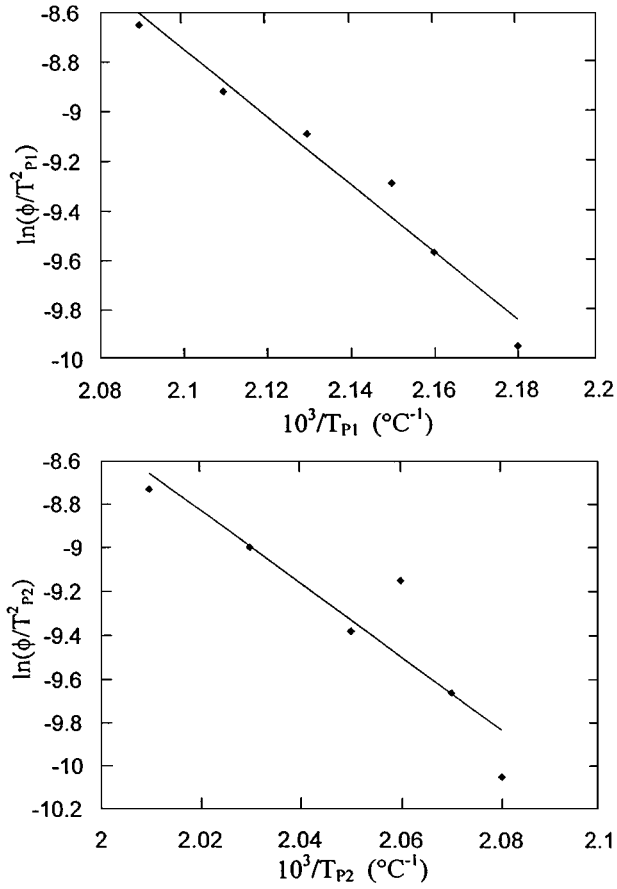

Figure 6 Plot of $\ln(\phi/T_p^2)$ vs. $10^3/T_p$ of $(85TeO_2 + 10TiO_2 + 5Fe_2O_3)$ glasses for the first and second crystallization peaks (T_{p1} and T_{p2}).

$\phi = 25\,^\circ$C/min) and at 485 °C (the second crystallization peak temperature for heating rate $\phi = 25\,^\circ$C/min). Fe_2O_3 is not detected in the XRD pattern and this could be due to its small ratio in the glass matrix (5 mol %) and the strong intensities of the Paratellurite TeO_2 and Titanium Tellurite ($TiTe_3O_8$) phases.

Fig. 9 shows the Infrared (IR) spectra of the as prepared $(85TeO_2 + 15TiO_2)$ glass sample and samples heat-treated at the first and second crystallization peaks for 30 min. It is observed that all spectra show the same characteristic bands. The bands of the as prepared glasses centered at 450, 630, 670, and 755 cm^{-1} are very broad due to the distribution of bond angles and lengths of the amorphous matrix. The characteristic IR

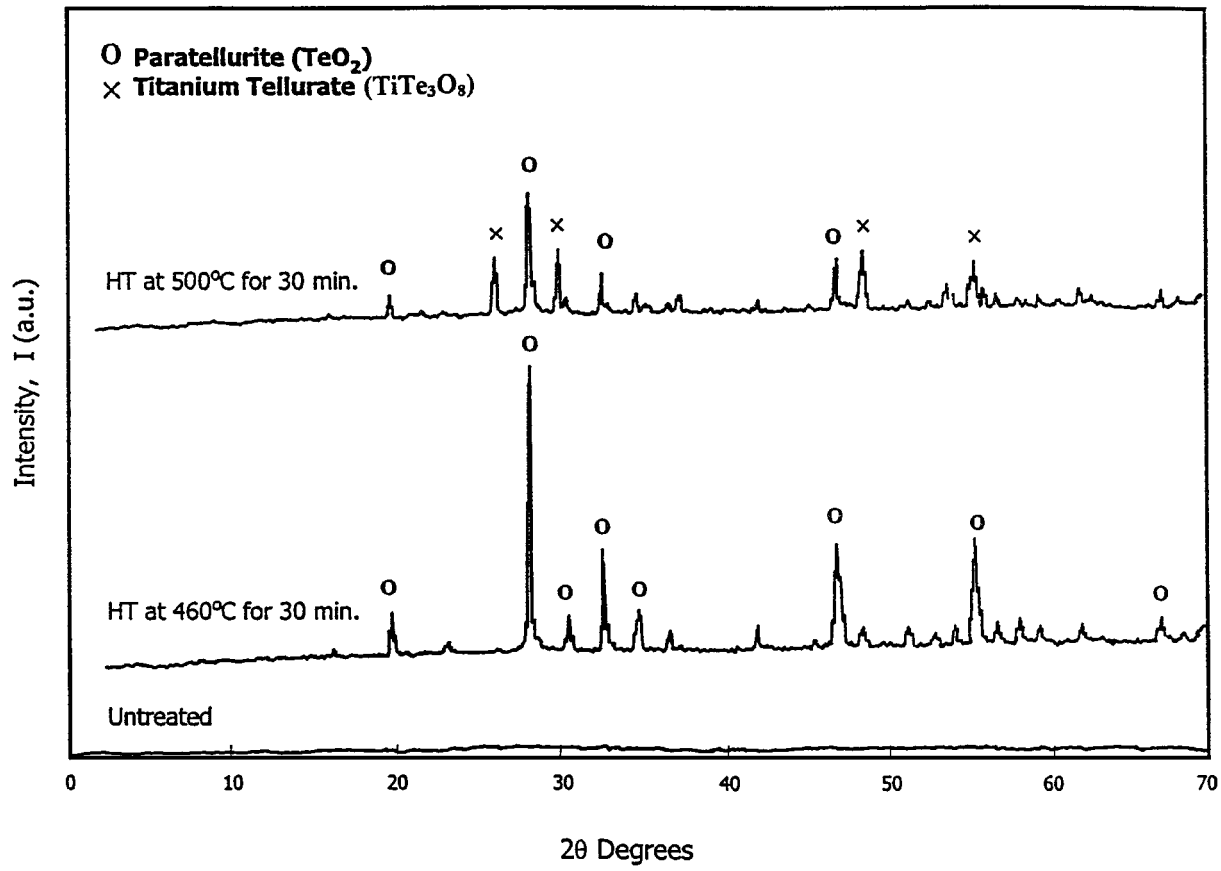

Figure 7 Powder X-ray diffraction patterns of ($85TeO_2 + 15TiO_2$) untreated and heat-treated glasses.

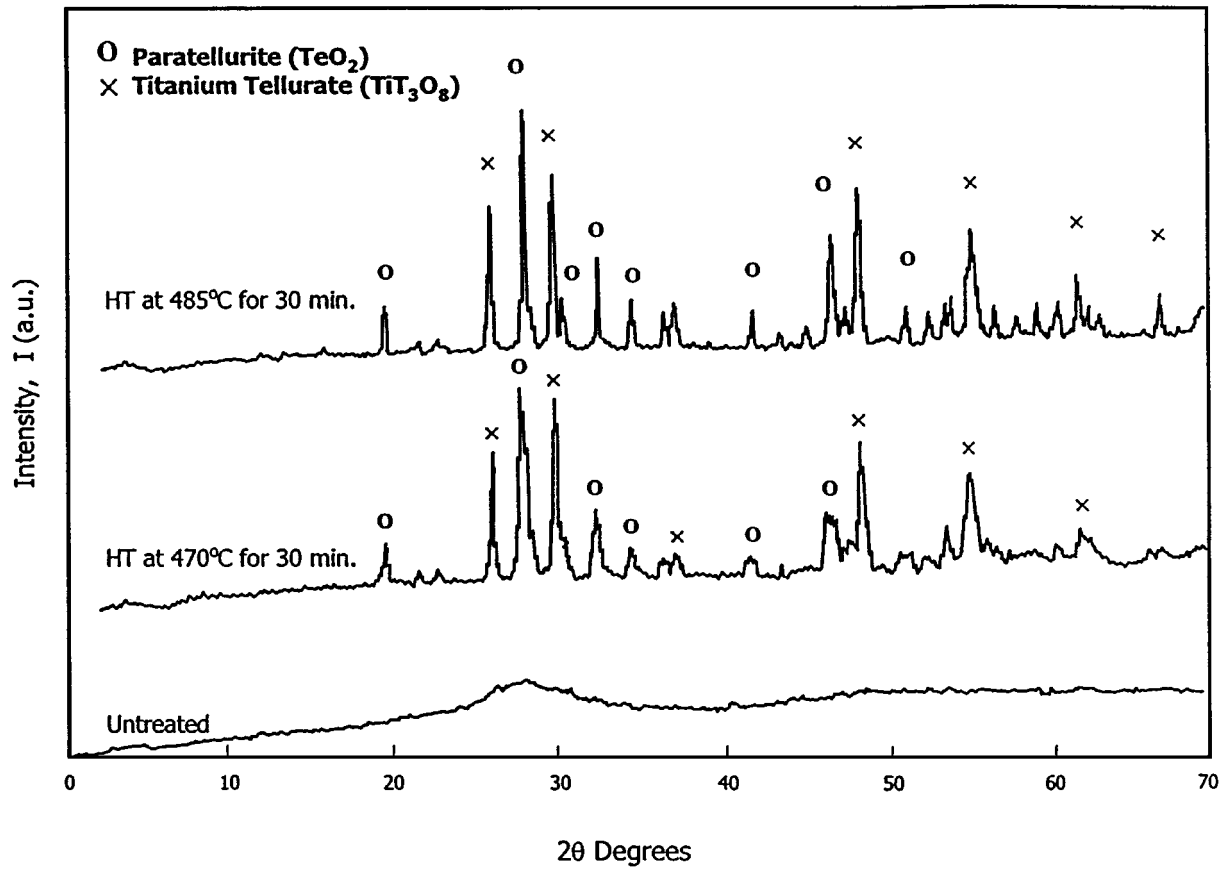

Figure 8 Powder X-ray diffraction patterns of ($85TeO_2 + 10TiO_2 + 5Fe_2O_3$) untreated and heat treated glasses.

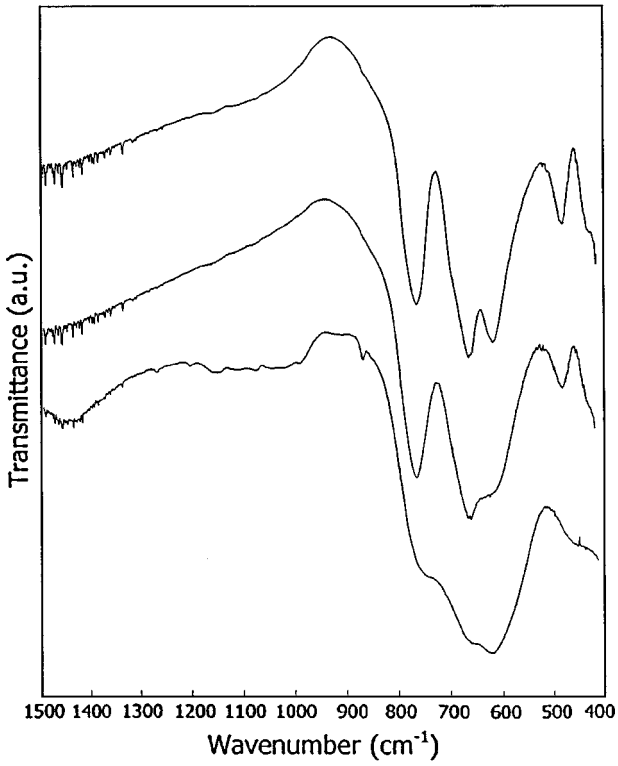

Figure 9 FTIR transmittance spectra of $(85TeO_2 + 15TiO_2)$ untreated and heat-treated glasses.

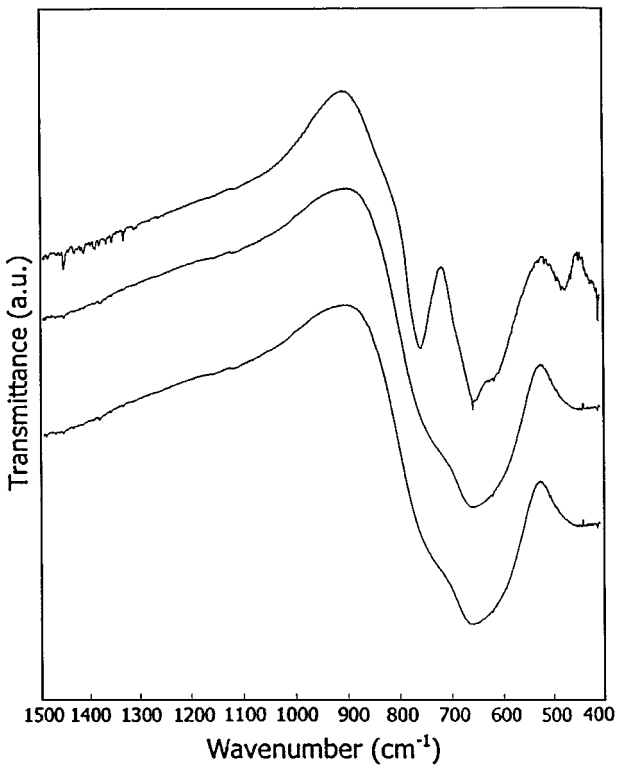

Figure 10 FTIR transmittance spectra of $(85TeO_2 + 10TiO_2 + 5Fe_2O_3)$ untreated and heat-treated glasses.

frequencies of crystalline TeO_2 are known to be at 635, 675, 714, and 780 cm^{-1} [2, 4, 24]. On comparison of the IR frequencies of crystalline TeO_2 and the IR spectrum of the untreated $(85TeO_2 + 15TiO_2)$ glasses, shown in Fig. 9, it is clear that the shoulder observed at 755 cm^{-1} in the glass spectrum is corresponding to the band at 780 cm^{-1} of crystalline TeO_2. The broad bands at 670 and 630 cm^{-1} are corresponding respectively to the two bands at 675 and 635 cm^{-1} of crystalline TeO_2 [2, 4, 24]. These modes observed for glasses are corresponding to the vibrational modes of trigonal bipyramids of crystalline TeO_2. The band centered at 450 cm^{-1} observed in the spectrum of the as prepared glasses is due to the Te-O-Ti stretching vibrations.

As shown in Fig. 9, upon heat treatment, the glass samples have been crystallized and the broad bands have been resolved into two sharp bands at 773 cm^{-1} and at 672 cm^{-1}, and relatively broad bands at 630 cm^{-1} and at 485 cm^{-1}. This suggests that these glasses are disordered version of TeO_4 trigonal bipyramids where the Te atoms are four fold coordinated. Fig. 10 shows the IR spectra of the untreated $(85TeO_2 + 10TiO_2 + 5Fe_2O_3)$ glasses, and glasses heat-treated at the first and second crystallization temperature for 30 min. The untreated and heat-treated glasses show the same characteristic bands observed for $(85TeO_2 + 15TiO_2)$ glasses as discussed in Fig. 9. Such similarity suggests that both glasses are disordered version of crystalline TeO_2.

4. Conclusions

Crystallization kinetics of the $(85TeO_2 + 15TiO_2)$ glasses and $(85TeO_2 + 10TiO_2 + 5Fe_2O_3)$ glasses have been studied and the activation energies of the glass transition and crystallization processes were determined. Two or three crystallization peaks have been observed in these Tellurite glasses and they were discussed in view of the polymorphic nature of crystalline TeO_2. Crystallized phases developed upon heat treatment of these glasses were identified by XRD. FTIR spectra of the heat-treated and untreated glasses showed them to be disordered versions of crystalline TeO_2 where the Te atoms are four fold coordinated.

References

1. T. NISHIDA, M. YAMADA, T. ICHII and Y. YAKASHIMA, *Jpn. J. App. Phys.* **30** (1991) 768.
2. I. SHALTOUT, YI TANG, R. BRAUNSTEIN and E. E. SHAISHA, *J. Phys. Chem. Solids* **57** (1996) 1223.
3. T. KOMATSU, H. TAWARAYAMA, H. MOHRI and K. MATUSITA, *J. Non. Cryst Solids* **135** (1991) 105.
4. I. SHALTOUT, YI TANG, R. BRAUNSTEIN and A. M. ABU-ELAZM, *J. Phys. Chem. Solids* **56** (1995) 141.
5. A. GHOSH, *J. App. Phys.* **64** (1988) 2652.
6. Y. SAKURAI and J. YAMAKI, *J. Elect. Chem. Soc.* **132** (1985) 512.
7. Y. HIMEI, Y. MIURA, T. NANBA and A. OSAKA, *J. Non. Cryst. Solids* **211** (1997) 64.
8. T. KOMATSU and K. SHIOYA, *ibid.* **209** (1997) 305.
9. Z. PAN and S. H. MORGAN, *ibid.* **210** (1997) 130.
10. T. KOMATSU, H. TAWARAYAMA, H. MOHRI and K. MATUSITA, *ibid.* **135** (1991) 105.
11. R. ELMALLAWANY, *J. Mat. Sci.: Mat. Elect.* **6** (1995) 1.
12. M. M. ELKHOLY, *ibid.* **6** (1995) 404.
13. C. S. RAY, *J. Amer. Ceram. Soc.* **74** (1991) 60.
14. X. J. XU, *ibid.* **74** (1991) 909.
15. A. MAROTTA, A. BURI and F. BRANDA, *Therm. Anal.* **21** (1981) 227.
16. Y. DIMITRIEV, V. DIMITROV and M. ARDUNOV, *J. Mat. Sci.* **18** (1983) 1353.

17. C. H. L. GOODMAN, *Glass. Tech.* **28** (1987) 11.
18. J. C. PHILIPS, *J. Non. Cryst. Solids* **35 36** (1980) 1157.
19. A. A. BAHGAT, I. I. SHALTOUT and A. M. ABU-ELAZM, *J. Non. Cryst. Solids* **150** (1992) 179.
20. E. E. SHAISHA, A. A. BAHGAT, A. I. SABRY and N. A. EISSA, *Phys. Chem. Glasses* **26** (1985) 91.
21. K. MATUSITA and S. SAKA, *ibid.* **38** (1980) 741.
22. YONG-KEUN LEE and SE-YOUNG CHOI, *J. Mat. Sci.* **32** (1997) 431.
23. S. MAHADEVAN, A. GIRIDHAR and A. K. SINGH, *J. Non. Cryst. Solids* **88** (1986) 11.
24. V. DIMITROV and M. ARANUDOV and Y. DIMITRIEV, *Manatsh Chem.* **115** (1984) 987.

Received 16 December 1998
and accepted 15 July 1999